Vibration Analysis of a Composite Plate with Delamination

Nabil Hassan Hadi
Assistant Professor
College of Engineering-University of Baghdad
email:nabilhha@yahoo.com

Basim Jameel Hamood
M. Sc. Student
College of Engineering-University of Baghdad
email:basimjameel@yahoo.com

ABSTRACT

The use of composite materials has vastly increased in recent years. Great interest is therefore developed in the damage detection of composites using non- destructive test methods. Several approaches have been applied to obtain information about the existence and location of the faults. This paper used the vibration response of a composite plate to detect and localize delamination defect based on the modal analysis. Experiments are conducted to validate the developed model. A two-dimensional finite element model for multi-layered composites with internal delamination is established. FEM program are built for plates under different boundary conditions. Natural frequencies and modal displacements of the intact and damaged multi-layer composite plates are subsequently analyzed for various samples. Also, composite plates are made for vibration testing and analysis and to comparison of the numerical and experimental results, shows good agreement between them.

Key words: composite plate, delamination, frequency response, finite element method, impact hummer.

تحليل الاهتزاز للوحة مركبة مع التبطين

نبيل حسن هادي
استاذ مساعد
كلية الهندسة-جامعة بغداد

باسم جميل حمود
طالب ماجستير
كلية الهندسة –جامعة بغداد

الخلاصة

لقد زاد استخدام المواد المركبة بشكل كبير في السنوات الأخيرة. مما اجتذب اهتماما كبيرا في الكشف عن العيب في المواد المركبة باستخدام طرق الاختبار غير المدمرة . وقد تم تطبيق عدة طرق للحصول على معلومات حول وجود العيب وتحديد موقعه. وتم استخدام استجابة الاهتزاز لوحة المركبة للكشف عن التبطين وتحديد موقعة استنادا إلى التردد الطبيعي. وتجرى التجارب للتحقق من صحة النموذج المطور . وتم انشاء نموذج ثنائي الأبعاد للمركبات متعددة الطبقات تحتوي على تبطين داخلي . ثم تبنى برنامج FEM باستعمل طريقة العناصر المحددة للوحات مختلفة في ظل ظروف حدية مختلفة. ويتم تحليل الترددات الطبيعية وشكل الازاحة للوحات مركب متعدد الطبقات سليمة و التالفة من برنامج FEM للحصول النتائج المطلوبة لعينات مختلفة. أيضا ، يتم إجراء اختبار الاهتزاز وتحليل و مقارنة النتائج العددية والعملية, وبينت النتائج تطابق جيد بينهما.

الكلمات الرئيسية : صفيحه مركبه ,والاستجابه الترديديه, طريقه العناصر المحدده, مطرقه الصدم.

1. INTRODUCTION

Laminated composite plate with reinforced fiber has lighter weight and higher ratios of strength and stiffness to weight, therefore it has been widely applied to many aeronautical and astronautically structures as well as architecture and light industry products. With the quality improvement and occurrence of many new kinds of composite materials, their applications have become more and more extensive. However, laminated composite structures are weak in withstanding shock and likely to be aging, and some damage, such as delamination and crack, may often occur during their usage. These disadvantages will lead to a deterioration of the performance and even failure of the composite materials. Any damage in a composite structure always starts from a very tiny extent and gradually cumulates to some degree that can arouse people's attention. However, when such damage in a structure reaches a notable level, a serious accident will be induced. Obviously, the early discovery of incipient damage and the continuously monitoring for the growth and location of damage are the most essential issues in automatic damage inspection of in-service composite structures **Gobin, et al., 2000.,**and **Takeda, 2000.** Delamination can be often pre-existing or generated during service life. For example, delamination often occur at stress free edges due to the mismatch of properties at ply interfaces and it can also be generated by external forces such as out of plane loading or impact during the service life. The existence of delamination not only alters the load carrying capacity of the structure, it can also affect its dynamic response. Thus detection and quantification of delamination is an important technology that must be addressed for the successful implementation and improved reliability of such structures. All types of damages in composite structures result in change in stiffness, strength and fatigue properties. Measurement of strength or fatigue properties during damage development is not feasible because destructive testing is required. However, stiffness reduction due to damage can be measured since damage directly affects structural response, which provides a promising method for identifying the occurrence, location and extent of the damage from measured structural dynamic characteristics. Existence of delamination causes reduction in natural frequencies and increase in vibratory damping. Although experimental investigations are often used to study these effects, damage simulation using an accurate and efficient modeling technique can be helpful in reducing the number of expensive experiments. Modeling and detection of delamination in composite structures has primarily been based on first-order shear deformation theory (FSDT), **Shen, and Grady, 2000.**

2. THEORY

2.1 Finite Element Formulation

A delaminated composite plate of length *a*, width *b* and thickness *h* consisting of *n* arbitrary number of anisotropic layers is considered as shown in **Fig. 1**. The layer details of the plate are shown in **Fig. 2**. The global coordinate system is considered with respect to the mid-plane of the plate with the Z-axis perpendicular to the X-Y plane and θ is the angle of fiber orientation, measured anticlockwise with respect to X-axis. In the present investigation, the delaminated composite plate is discretized in to a mesh of 5×5 with total 25 elements. An nine nodes two dimensional quadratic isoperimetric element having five degrees of freedom (u^0, v^0, w^0, θ_x, θ_y) per node is chosen.

2.1.1 Displacement field and shape functions

The displacement field of any point at a distance z from the mid surface is assumed to be in the form of:

$$u(x,y,z)=u^0(x,y)+z\theta_x(x,y) \tag{1}$$

$$v(x,y,z)=v^0(x,y)+z\theta_y(x,y) \tag{2}$$

$$w(x,y,z)=w^0(x,y) \tag{3}$$

where *u, v, w* are displacements in the *x,y,z* directions respectively for any point, u^0,v^0 , w^0 are those at the middle plane of the plate. θ_x, θ_y are the rotations of the cross section normal to the *y* and *x* axis respectively. The middle plane of the plate is considered as the reference plane of the plate. The mid plane strains of the laminate are given by:

$$\varepsilon_{xx}^0=u_{,x}^0;\quad \varepsilon_{yy}^0=v_{,y}^0;\quad \gamma_{xy}^0=u_{,y}^0+v_{,x}^0;\quad \gamma_{xz}^0=\theta_x+w_{,x};\quad \gamma_{yz}^0=\theta_y+w_{,y} \tag{4}$$

Assuming small deformations, the generalized linear in-plane strains of the laminate at a distance *z* from the mid-surface are expressed as:

$$\{\varepsilon_{xx}\quad \varepsilon_{yy}\quad \gamma_{xy}\quad \gamma_{xz}\quad \gamma_{yz}\}^T=\{\varepsilon_{xx}^0\quad \varepsilon_{yy}^0\quad \gamma_{xy}^0\quad \gamma_{xz}^0\quad \gamma_{yz}^0\}^T+z\{k_{xx}\quad k_{yy}\quad k_{xy}\quad k_{xz}\quad k_{yz}\}^T \tag{5}$$

Where $$\begin{Bmatrix}\varepsilon_{xx}^0\\ \varepsilon_{yy}^0\\ \gamma_{xy}^0\\ \gamma_{xz}^0\\ \gamma_{yz}^0\end{Bmatrix}=\begin{Bmatrix}\left(\frac{\partial u^0}{\partial x}\right)\\ \left(\frac{\partial v^0}{\partial y}\right)\\ \left(\frac{\partial u^0}{\partial y}+\frac{\partial v^0}{\partial x}\right)\\ \theta_x+\frac{\partial w^0}{\partial x}\\ \theta_y+\frac{\partial w^0}{\partial y}\end{Bmatrix}$$ and $$\begin{Bmatrix}k_{xx}^0\\ k_{yy}^0\\ k_{xy}^0\\ k_{xz}^0\\ k_{yz}^0\end{Bmatrix}=\begin{Bmatrix}\left(\frac{\partial \theta_x}{\partial x}\right)\\ \left(\frac{\partial \theta_y}{\partial y}\right)\\ \left(\frac{\partial \theta_x}{\partial y}+\frac{\partial \theta_y}{\partial x}\right)\\ 0\\ 0\end{Bmatrix}$$

where ε^0_{xx}, ε^0_{yy}, γ^0_{xy} are the mid-plane strains and k_{xx} k_{yy} k_{xy} are the curvatures of the laminated plate .

The element has 4 corner nodes, 4 mid side nodes and mid element node. In the displacement model, simple functions are assumed to approximate the displacements for each element. For the present isoperimetric element, the shape functions which are used to represent the geometry as well as the displacements within the element are expressed by the shape functions N_i.

$$x=\sum_{i=1}^{9}N_i x_i \qquad y=\sum_{i=1}^{9}N_i y_i \qquad u=\sum_{i=1}^{9}N_i u_i^0 \qquad v^0=\sum_{i=1}^{9}N_i v_i^0$$

$$w=\sum_{i=1}^{9}N_i w_i \qquad \theta_x=\sum_{i=1}^{9}N_i\theta_{xi} \qquad \theta_y=\sum_{i=1}^{9}N_i\theta_{yi} \tag{6}$$

where x_i, y_i ,are the co-ordinates of the i^{th} node and u_i^0, v_i^0,w_i, θ_{xi}, θ_{yi} are the displacement functions for different nodes.
Ni for different nodes as shown in **Fig. 3** is defined as,
At corner nodes (i.e. for node 1, 3, 5, 7)

$$N_i=\tfrac{1}{4}(1+\xi\xi_i)(1+\eta\eta_i)(\xi\xi_i+\eta\eta_i-1)$$

At middle nodes (i.e. for nodes 2, 6)

$$N_i=\tfrac{1}{2}(1-\xi^2)(1+\eta\eta_i)$$

At middle nodes (i.e. for nodes 4, 8)

$$N_i=\tfrac{1}{2}(1+\xi\xi_i)(1-\eta^2)$$

At middle element (i.e. for node 9)

$$N_9=(1-\xi^2)(1-\eta^2)$$

Where ξ and η are the local isoperimetric co-ordinates of the element and ξ_i and η_i are the respective values at node i. The correctness of the shape function N_i is checked from the relations

$$\sum N_i=1 \qquad \sum N_i,\xi=0 \qquad \sum N_i,\eta=0 \tag{7}$$

The derivatives of the shape functions N_i with respect to x and y are expressed in terms of their partial derivatives with respect to ξ and η by the relationships:

$$\begin{Bmatrix}\dfrac{\partial N_i}{\partial x}\\ \dfrac{\partial N_i}{\partial y}\end{Bmatrix}=\begin{Bmatrix}\dfrac{\partial\xi}{\partial x} & \dfrac{\partial\eta}{\partial x}\\ \dfrac{\partial\xi}{\partial y} & \dfrac{\partial\eta}{\partial y}\end{Bmatrix}\begin{Bmatrix}\dfrac{\partial N_i}{\partial\xi}\\ \dfrac{\partial N_i}{\partial\eta}\end{Bmatrix}$$

$$\begin{bmatrix}N_{i,x}\\ N_{i,y}\end{bmatrix}=[J]^{-1}\begin{bmatrix}N_{i,\xi}\\ N_{i,\eta}\end{bmatrix} \tag{8}$$

Where $[J]=\begin{bmatrix}x,_\xi & y,_\xi\\ x,_\eta & y,_\eta\end{bmatrix}=\begin{bmatrix}\sum N_{i,\xi}x_i & \sum N_{i,\xi}y_i\\ \sum N_{i,\eta}x_i & \sum N_{i,\eta}y_i\end{bmatrix}$ is the Jacobin matrix.

2.1.2 Stress strain relations

A micromechanical analysis is carried out to establish the relationship between the forces and strains of a laminate. The elastic behavior of each lamina is essentially two dimensional and orthotropic in nature. So the elastic constants for the composite lamina.

2.1.3 Strain displacement relations

Strain displacement is used throughout the structural analysis. It is used to derive the elastic stiffness matrix.

The strains are defined as.

$$\begin{Bmatrix}\sigma_1\\ \sigma_2\\ \sigma_6\\ \sigma_5\\ \sigma_4\end{Bmatrix}^k = \begin{bmatrix}\overline{Q}_{11} & \overline{Q}_{12} & \overline{Q}_{16} & 0 & 0\\ \overline{Q}_{12} & \overline{Q}_{22} & \overline{Q}_{26} & 0 & 0\\ \overline{Q}_{16} & \overline{Q}_{26} & \overline{Q}_{66} & 0 & 0\\ 0 & 0 & 0 & \overline{Q}_{55} & \overline{Q}_{45}\\ 0 & 0 & 0 & \overline{Q}_{45} & \overline{Q}_{44}\end{bmatrix}^k \begin{bmatrix}\begin{Bmatrix}\varepsilon_1\\ \varepsilon_2\\ \varepsilon_6\\ \varepsilon_5\\ \varepsilon_4\end{Bmatrix}^k\end{bmatrix} \tag{9}$$

The strain can be described in term of displacements as

$$\{\varepsilon\} = [B]\{de\} \tag{10}$$

Where $\{de\} = [u_1 v_1 w_1 \phi_{11} \phi_{21} \cdots\cdots\cdots\cdots u_9 v_9 w_9 \phi_{19} \phi_{29}]^T$

$$[B] = [[B_1].....[B_8][B_9]]$$

$$[B_i] = \begin{bmatrix}\frac{\partial N_i}{\partial \alpha} & 0 & 0 & 0 & 0\\ 0 & \frac{\partial N_i}{\partial \beta} & 0 & 0 & 0\\ \frac{\partial N_i}{\partial \beta} & \frac{\partial N_i}{\partial \alpha} & 0 & 0 & 0\\ 0 & 0 & 0 & \frac{\partial N_i}{\partial \alpha} & 0\\ 0 & 0 & 0 & 0 & \frac{\partial N_i}{\partial \beta}\\ 0 & 0 & 0 & \frac{\partial N_i}{\partial \beta} & \frac{\partial N_i}{\partial \alpha}\\ 0 & 0 & \frac{\partial N_i}{\partial \alpha} & N_i & 0\\ 0 & 0 & \frac{\partial N_i}{\partial \beta} & 0 & N_i\end{bmatrix} \tag{11}$$

2.1.4 Derivation of element matrices

2.1.4.1 Elastic stiffness matrix

The potential energy of deformation for the element is given by

$$U_e = \frac{1}{2}\int\int \{\varepsilon\}^T [\sigma] dA \tag{12}$$

$$\{\varepsilon\} = \left\{\varepsilon_1^0 \varepsilon_2^0 \varepsilon_6^0 k_1^0 k_2^0 k_6^0 \gamma_5^0 \gamma_4^0\right\}^T \tag{13}$$

Where $\{\varepsilon\} = [B]\{d_e\} = [[B_1].....[B_8][B_9]]\{d_e\}$ (14)

With $\{de\} = \left[u_1^0 v_1^0 w_1 \phi_1^1 \phi_2^1 \cdots\cdots\cdots\cdots u_9^0 v_9^0 w_9 \phi_1^9 \phi_2^9\right]^T$ (15)

Then $U_e = \frac{1}{2}\int\int \{d_e\}^T [B]^T [D][B]\{d_e\} dxdy = \frac{1}{2}\{d_e\}^T [K_e]\{d_e\}$ (16)

Where the element stiffness matrix

$$[K_e] = \int_{-1}^{1}\int_{-1}^{1} [B]^T [D][B] J\left| d\xi d\eta \right. \tag{17}$$

[B] is called the strain displacement matrix.

In Eq. (17) $[B_i] = \sum_{i=1}^{9} \begin{bmatrix} N_{i,x} & 0 & 0 & 0 & 0 \\ 0 & N_{i,y} & 0 & 0 & 0 \\ N_{i,y} & N_{i,x} & 0 & 0 & 0 \\ 0 & 0 & 0 & N_{i,x} & 0 \\ 0 & 0 & 0 & 0 & N_{i,y} \\ 0 & 0 & 0 & N_{i,y} & N_{i,x} \\ 0 & 0 & N_{i,x} & N_i & 0 \\ 0 & 0 & N_{i,y} & 0 & N_i \end{bmatrix}$

$\left|J\right| d\xi d\eta$, is the determinant of the Jacobian matrix. The element stiffness matrix can be expressed in local natural co-ordinates of the element. The integration of Eq. (17) is carried out using the Gauss quadrature method.

2.1.4.2 Consistent mass matrix

The consistent element mass matrix [*Me*] is expressed as:

$$[M_e] = \int_{-1}^{1}\int_{-1}^{1} [N]^T [P][N] J\left| d\xi d\eta \right. \tag{18}$$

Where [*N*], the shape function matrix and [*P*], the inertia matrix

$$[N]=\begin{bmatrix} N_i & 0 & 0 & 0 & 0 \\ 0 & N_i & 0 & 0 & 0 \\ 0 & 0 & N_i & 0 & 0 \\ 0 & 0 & 0 & N_i & 0 \\ 0 & 0 & 0 & 0 & N_i \end{bmatrix} \quad \text{i=1 to 9} \quad , \quad [P]=\begin{bmatrix} P_1 & 0 & 0 & P_2 & 0 \\ 0 & P_1 & 0 & 0 & P_2 \\ 0 & 0 & P_1 & 0 & 0 \\ P_2 & 0 & 0 & P_3 & 0 \\ 0 & P_2 & 0 & 0 & P_3 \end{bmatrix} \tag{19}$$

Where $(P_1, P_2, P_3) = \sum_{i=1}^{9} \int_{z_{k-1}}^{k} (\rho)_k (1, z, z^2) dz$

2.2 Delamination Modeling

A simple two dimensional single delamination model proposed by ,**Gim C.K.1994.** was extended by ,**Mohammad F.Aly.2010** for the vibration of delaminated composite panels. In the present analysis, it is further extended for static and dynamic stability analysis under in-plane uniaxial periodic forces by multiple delamination modelling. In order to satisfy the compatibility and equilibrium requirements at the common delamination boundary, it is assumed that the in-plane displacement, transverse displacement and rotation at a common node for all the three sublaminates including the original one are identical applying multiple constraint condition at any arbitrary delamination boundary. It can be applicable to any general case of a laminated composite plate having multiple delamination at any arbitrary location. Here, the delaminated area is assumed as the interface of two separate sub laminates bonded together along the delamination surface.

Typical composite plate of uniform thickness *'h'* with '*n'* number of layers and '*p'* number of arbitrarily located delamination is considered for the analysis as shown in **Fig. 4**. The principal material axes of each layer are arbitrarily oriented with respect to the mid-plane of the plate as shown in **Fig. 5**.

Considering the sub-laminates as a separate plate, the displacement field within it is expressed as:

$$u_s = u_s^0 + (z - z_s^0)\theta_{xs}, \quad v_s = v_s^0 + (z - z_s^0)\theta_{ys} \tag{20}$$

Where u_s^0 and v_s^0 are the mid-plane displacements of the s^{th} sub-laminate along *x* and *y* direction and z_s^0 is distance between mid-plane of s^{th} sub-laminate and the mid-plane of the laminate in *z* direction

The mid-plane strains of the sub-laminate are:

$$\{\varepsilon_{xx}^0 \quad \varepsilon_{yy}^0 \quad \gamma_{xy}^0\}_s^T = \left\{ \frac{\partial u_s^0}{\partial x} \quad \frac{\partial v_s^0}{\partial y} \quad \frac{\partial u_s^0}{\partial y} + \frac{\partial v_s^0}{\partial x} \right\}^T \tag{21}$$

From Eq. (21) the strain components within the sub-laminate *s* can be expressed as:

$$\{\varepsilon_{xx}^0 \quad \varepsilon_{yy}^0 \quad \gamma_{xy}^0\}_s^T = \left\{ \frac{\partial u_s}{\partial x} \quad \frac{\partial v_s}{\partial y} \quad \frac{\partial u_s}{\partial y} + \frac{\partial v_s}{\partial x} \right\}^T$$

$$= \left\{ \frac{\partial u_s^0}{\partial x} \quad \frac{\partial v_s^0}{\partial y} \quad \frac{\partial u_s^0}{\partial y} + \frac{\partial v_s^0}{\partial x} \right\}^T + \left(z - z_s^0\right) \left\{ \frac{\partial \theta_x}{\partial x} \quad \frac{\partial \theta_y}{\partial y} \quad \frac{\partial \theta_x}{\partial y} + \frac{\partial \theta_y}{\partial x} \right\}^T$$

$$= \left\{ \varepsilon_{xx}^0 \quad \varepsilon_{yy}^0 \quad \gamma_{xy}^0 \right\}_s^T + \left(z - z_s^0\right) \left\{ k_{xx} \quad k_{yy} \quad k_{xy} \right\}_s^T \tag{22}$$

In order to satisfy the compatibility and equilibrium requirements at the common delamination boundary, it is assumed that the in-plane displacements, transverse displacement and rotations at a common node for all the three sub-laminates including the original one as shown in **Fig.6**, are identical. Applying multiple constraint condition at any arbitrary delamination boundary *c*, the in-plane displacements at *'c'* at a distance *'z'* from the mid-plane of the laminate can be written as:

$$u_c = u^0 + z\theta_x \quad , \quad v_c = v^0 + z\theta_y$$

From Eq. (20), the displacement at any point, *c* is given by:

$$u_{sc} = u_s^0 + \left(z - z_s^0\right)\theta_x \quad , \quad v_{sc} = v_s^0 + \left(z - z_s^0\right)\theta_y$$

Equating u_c with u_{sc} and v_c with v_{sc}, the mid-plane displacements of the sub-laminate can be expressed in the form of the mid-plane displacements(u^0, v^0) of the original un-delaminated laminate as,

$$u_s^0 = u^0 + z_s^0\theta_x \quad , \quad v_s^0 = v^0 + z_s^0\theta_y \tag{23}$$

From Eq. (23), the mid-plane strain components of the s^{th} sub-laminate can be derived as:

$$\left\{ \varepsilon_{xx}^0 \quad \varepsilon_{yy}^0 \quad \gamma_{xy}^0 \right\}_s^T = \left\{ \varepsilon_{xx}^0 \quad \varepsilon_{yy}^0 \quad \gamma_{xy}^0 \right\}^T + z_s^0 \left\{ k_{xx} \quad k_{yy} \quad k_{xy} \right\}^T \tag{24}$$

The strain components within the sub-laminate can be written as:

$$\left\{ \varepsilon_{xx} \quad \varepsilon_{yy} \quad \gamma_{xy} \right\}_s^T = \left\{ \varepsilon_{xx}^0 \quad \varepsilon_{yy}^0 \quad \gamma_{xy}^0 \right\}_s^T + \left(z - z_s^0\right) \left\{ k_{xx} \quad k_{yy} \quad k_{xy} \right\}^T$$

$$= \left\{ \varepsilon_{xx}^0 \quad \varepsilon_{yy}^0 \quad \gamma_{xy}^0 \right\}^T + z_s^0 \left\{ k_{xx} \quad k_{yy} \quad k_{xy} \right\}^T + \left(z - z_s^0\right) \left\{ k_{xx} \quad k_{yy} \quad k_{xy} \right\}^T \tag{25}$$

For any lamina of s^{th} sub-laminate, the in-plane and shear stresses are found from the following relations

$$\begin{Bmatrix} \sigma_{xx} \\ \sigma_{yy} \\ \tau_{xy} \end{Bmatrix} = \begin{bmatrix} \overline{Q}_{11} & \overline{Q}_{12} & \overline{Q}_{16} \\ \overline{Q}_{12} & \overline{Q}_{22} & \overline{Q}_{26} \\ \overline{Q}_{16} & \overline{Q}_{26} & \overline{Q}_{66} \end{bmatrix} \begin{Bmatrix} \varepsilon_{xx} \\ \varepsilon_{yy} \\ \gamma_{xy} \end{Bmatrix}_s \tag{26}$$

$$\begin{Bmatrix}\tau_{xz}\\ \tau_{yz}\end{Bmatrix}=\begin{bmatrix}\overline{Q}_{44} & \overline{Q}_{45}\\ \overline{Q}_{45} & \overline{Q}_{55}\end{bmatrix}\begin{bmatrix}\gamma_{xz}\\ \gamma_{yz}\end{bmatrix}_s \tag{27}$$

Where σ_{xx} and σ_{yy} are the normal stresses along x and y directions respectively and τ_{xz} and τ_{yz} are the shear stresses in xz, yz planes respectively.

Integrating these stresses over the thickness of the sub-laminate, the stress and moment resultants of the sub-laminate are derived which lead to the elasticity matrix of the s^{th} sub-laminate $[D]_s$ in the form

$$[D]_s=\begin{bmatrix}A_{ij} & z_s^0A_{ij}+B_{ij} & 0\\ B_{ij} & z_s^0B_{ij}+D_{ij} & 0\\ 0 & 0 & S_{ij}\end{bmatrix} \tag{28}$$

$[D]_s$ is the elasticity matrix of the s^{th} sub-laminate

Where, $\left[A_{ij}\right]_s=\int_{-\frac{h_s}{2}+z_s^0}^{\frac{h_s}{2}+z_s^0}\left[\overline{Q}_{ij}\right]_s dz$ and $\left[B_{ij}\right]_s=\int_{-\frac{h_s}{2}+z_s^0}^{\frac{h_s}{2}+z_s^0}\left[\overline{Q}_{ij}\right]_s\left(z-z_s^0\right)dz=\int_{-\frac{h_s}{2}+z_s^0}^{\frac{h_s}{2}+z_s^0}\left[\overline{Q}_{ij}\right]_s zdz-z_s^0\left[A_{ij}\right]_s$

$$\left[D_{ij}\right]_s=\int_{-\frac{h_s}{2}+z_s^0}^{\frac{h_s}{2}+z_s^0}\left[\overline{Q}_{ij}\right]_s\left(z-z_s^0\right)^2dz=\int_{-\frac{h_s}{2}+z_s^0}^{\frac{h_s}{2}+z_s^0}\left[\overline{Q}_{ij}\right]_s\left[z^2+\left(z_s^0\right)^2-2zz_s^0\right]dz=\int_{-\frac{h_s}{2}+z_s^0}^{\frac{h_s}{2}+z_s^0}\left[\overline{Q}_{ij}\right]_s z^2dz$$

$$-2z_s^0\int_{-\frac{h_s}{2}+z_s^0}^{\frac{h_s}{2}+z_s^0}\left[\overline{Q}_{ij}\right]_s zdz+\left(z_s^0\right)^2\left[A_{ij}\right]_s \qquad \text{for i, j = 1, 2, 6}$$

$$\left[S_{ij}\right]_s=\int_{-\frac{h_s}{2}+z_s^0}^{\frac{h_s}{2}+z_s^0}\left[\overline{Q}_{ij}\right]_s dz \qquad \text{for i,j =4,5}$$

The in-plane stress and moment resultants for the s^{th} sub-laminate can be expressed in a generalized manner as:

$$\begin{Bmatrix} N_{xx} \\ N_{yy} \\ N_{xy} \\ M_{xx} \\ M_{yy} \\ M_{xy} \end{Bmatrix} = \begin{bmatrix} A_{11} & A_{12} & A_{16} & z_s^0 A_{11} + B_{11} & z_s^0 A_{12} + B_{12} & z_s^0 A_{16} + B_{16} \\ A_{12} & A_{22} & A_{26} & z_s^0 A_{12} + B_{12} & z_s^0 A_{22} + B_{22} & z_s^0 A_{26} + B_{26} \\ A_{16} & A_{26} & A_{66} & z_s^0 A_{16} + B_{16} & z_s^0 A_{26} + B_{26} & z_s^0 A_{66} + B_{66} \\ B_{11} & B_{12} & B_{16} & z_s^0 B_{11} + D_{11} & z_s^0 B_{12} + D_{12} & z_s^0 B_{16} + D_{16} \\ B_{12} & B_{22} & B_{26} & z_s^0 B_{12} + D_{12} & z_s^0 B_{22} + D_{22} & z_s^0 B_{26} + D_{26} \\ B_{16} & B_{26} & B_{66} & z_s^0 B_{16} + D_{16} & z_s^0 B_{26} + D_{26} & z_s^0 B_{66} + D_{66} \end{bmatrix} \begin{Bmatrix} \varepsilon_{xx}^0 \\ \varepsilon_{yy}^0 \\ \varepsilon_{xy}^0 \\ k_{xx} \\ k_{yy} \\ k_{xy} \end{Bmatrix}_s \tag{29}$$

Similarly, the transverse shear resultants for the s^{th} sub-laminate are presented as

$$\begin{Bmatrix} Q_{xz} \\ Q_{yz} \end{Bmatrix}_s = \begin{bmatrix} S_{44} & S_{45} \\ S_{45} & S_{55} \end{bmatrix}_s \begin{bmatrix} \gamma_{xz} \\ \gamma_{yz} \end{bmatrix} \tag{30}$$

After finding the elastic stiffness matrices separately for different sub-laminates along the thickness, the sum of all the sub-laminate stiffness's represents the resultant stiffness matrix.

2.3 Characteristics of the Reinforcement-Matrix Mixture

The mechanical properties of constituents of the test specimens, E-glass woven roving fibers and polyester matrix are listed in **Table 1**.

The material elastic properties of the lamina of test specimens are determined experimentally. These properties are Young's moduli (E_1 – in direction 1, E_2 – in direction 2, E_3 – in direction 3), Poisson's ratios ($\upsilon_{12}, \upsilon_{13}$, and υ_{23}), in plane shear modulus (G_{12}) and transverse shear moduli (G_{13} and G_{23}). This figure defines the material principle axes for a typical woven fiber reinforced lamina. Axis 1 is along the fiber length and represents the longitudinal direction of the lamina; axes 2 and 3 represent the transverse in-plane and through the thickness directions respectively.

Some of the elastic constants of the woven fabric composite material are experimentally estimated (E_1, E_2, υ_{12}). The others are estimated by using the relations which are based on elastic constants of the unidirectional specimens. Young's modulus and the Poisson's ratio of the fill and warp directions are calculated by using the three-point bending test, and the interface strain meter is to calculate the Poisson ratio (υ_{12}) from a program using the computer.

2.3.1 Unidirectional ply

The elastic constants of the unidirectional composite are calculated using the simple rule of mixtures by the relations of Eq. (31), **Metin Aydogdu. 2007.** and the results are listed in **Table 2.**

$$E_1 = E_f \nu_f + E_m (1 - \nu_f)$$

$$E_2 = E_m \left[\frac{E_f + E_m + \nu_f (E_f - E_m)}{E_f + E_m - \nu_f (E_f - E_m)} \right]$$

$$\upsilon_{12} = \upsilon_f \nu_f + \upsilon_m (1-\nu_f)$$

$$\upsilon_{23} = \left[\upsilon_f \nu_f + \upsilon_m (1-\nu_f)\right]\left[\frac{1+\upsilon_m - \upsilon_{12}\frac{E_m}{E_1}}{1-\upsilon_m^2 + \upsilon_m \upsilon_{12}\frac{E_m}{E_1}}\right]$$

$$G_{12} = G_m\left[\frac{G_f + G_m + \nu_f (G_f - G_m)}{G_f + G_m - \nu_f (G_f - G_m)}\right]$$

$$G_{23} = \frac{E_2}{2(1+\upsilon_{23})} \quad (31)$$

Where indices *m* and *f* denote matrix and fiber, respectively.

2.3.2 Woven fabrics

The elastic constants of the woven fabric composite material are estimated by using the tensile test device and the relation of Eq. (32) **D.Gay etal.2003** and the results are listed in **Table 3.**

- One is called the warp and,
- The other is called the fill (or weft) direction.

The fibers are woven together, which means the fill yarns pass over and under the warp yarns, following a fixed pattern. **Fig. 7** shows a plain weave where each fill goes over a warp yarn then under a warp yarn and so on.

The fabric layer is replaced by one single anisotropic layer, x being along the warp direction and y along the fill direction (see **Fig. 7**). One can therefore obtain **D.Gay etal.2003.**

$$E_{1w} = k.E_1 + (1-k)E_2$$

$$E_{2w} = (1-k)E_1 + k.E_2$$

$$G_{12w} = G_{12}$$

$$\upsilon_{12w} = \frac{\upsilon_{12}}{(k + (1-k)\frac{E_1}{E_2})} \quad (32)$$

Where $k = \frac{n_1}{n_1 + n_2}$, n_1=number of warp yarns per meter, n_2= number of fill yarns per meter. And, E_{1w}, E_{2w} ,G_{12w} , and υ_{12w} are mechanical properties of woven fabrics in 1 and 2-directions; and E_1, E_2, G_{12}, G_{23}, υ_{12} , and ν_{23} as in Eq. (31).

The stiffness obtained with a woven fabric is less than what is observed if one were to superpose two cross plies of unidirectional. This is due to the curvature of the fibers during the weaving operation. This curvature makes the woven fabric more deformable than the two cross

plies when subjected to the same loading. (There exist fabrics that are of "high modulus" where the unidirectional layers are not connected with each other by weaving. The unidirectional plies are held together by stitching fine threads of glass or polymer).

2.4 Modeling Assumptions

In this study, 8-layer Glass fiber Polyester resin laminated rectangular composite plates (325×325 mm^2) with a total thickness of 4 mm are examined.

The ply orientations are (0,90,0,90,0,90,0,90); the material constants are shown in **Table 1**.

Three plates are considered including an intact plate (plate A) and two damaged plates B and C. Plates B & C have delamination at **Fig. 8** in mid-plane with the size 50×50 mm; plate .Coordinates x and y are measured from the corner of the plate as the origin**.**

3. RESULTS

3.1 Delamination Effects on Natural Frequencies

In the present investigation, both the numerical computation and experimental study are carried out for an eight-layered $[0/90]_4$ woven glass fiber/polyester resin composite plate. The geometrical dimensions of the woven composite plates are: length, a =350 mm width, b = 350 mm, thickness, h = 3.25 mm. The material properties of the woven glass fiber/polyester resin composite plates are considered as given in **Table 3**. Square size delamination was introduced at the mid-plane as shown in **Fig. 8**. In this study, the effects of delamination area, boundary conditions, fiber orientations and number of layers on the natural frequencies are investigated.

Tables 4, 5, 6 and 7 give a comparison of the first five frequencies which is between experimental work and numerical work of the four woven laminated plate with different boundary conditions .These tables show good (harmonies) agreements at the first mode obtained between experimental and numerical works. The deviations for the numerical results and the experimental method are due to some possible measurement errors that can be pointed out such factors as: measurement noise, different positions of the accelerometers and their mass, non-uniformity in specimens' properties (voids, variations in thickness, non-uniform surface finishing). Such factors are not taken into account during the numerical analysis, since the model considers the specimen perfect entirely with homogeneous properties, which rarely occurs in the practice. Another aspect has to be considered is that the input properties in the model came from the application of the rule of mixture and it does not take into account the effects of fiber matrix interface as well as the irregular distribution of resin on the fibers. Also, the computational numerical program does not allow for the consideration of fibers interweaving presented in the fabric use.

3.2 Delamination Effects on Mode Shapes

The results of FEM analysis show the delamination regions clearly **Fig. 9**. The conducted analysis demonstrates that the delamination-induced changes of plate parameters mode

3.3 Effect of Number of Layer

Table 8 shows the effect of the number of layer (with the same thickness) on natural frequency with four boundary condition all sides clamped (CCCC), all sides simple supported (SSSS), cantilever plate (CFFF) and all sides free (FFFF), under step uniform dynamic loading. For (CCCC), shows the effect of the number of layer the natural frequency decreases with the increase number of layer from(1 to 2) with a decreasing percentage (0.88 %), increase when

number of layer increases from (2 to 3) with a percentage of (0.85 %), decreases with the increase number of layer from(3 to 4) with a decreasing percentage of (0.54 %), increase when number of layer increase from (4 to 5) with percentage (0.38 %), decreases with the increase number of layer from(5 to 6) with decreasing percentage (0.32 %), increase when number of layer increase from (6to 7) with percentage (0.25 %), decreases with the increase number of layer from(7 to 8) with decreasing percentage (0.23 %), for (SSSS), shows the effect of the number of layer the frequency response increases with the increase number of layer from(1 to 2) with percentage (4.67 %), decreases when number of layer increase from (2 to 3) with decreasing percentage (4.06 %), increases with the increase number of layer from(3 to 4) with percentage (4.91 %), decreases when number of layer increase from (4 to 5) with decreasing percentage (2.83 %), increases with the increase number of layer from(5 to 6) with percentage (3.04 %), decreases when number of layer increase from (6 to 7) with decreasing percentage (2.10 %), increase with the increase number of layer from(7 to 8) with percentage (2.18 %), for (CFFF), show the effect of the number of layer the frequency response decreases with the increase number of layer from(1 to 2) with decreasing percentage (7.25 %), increase when number of layer increase from (2 to 3) with percentage (7.45 %), decreases with the increase number of layer from(3 to 4) with decreasing percentage (5.44 %), increase when number of layer increase from (4 to 5) with percentage (3.97 %), decreases with the increase number of layer from(5 to 6) with decreasing percentage (3.55 %), increase when number of layer increase from (6 to 7) with percentage (2.78 %), decreases with the increase number of layer from(7 to 8) with decreasing percentage (2.61 %), for (FFFF), shows the effect of the number of layer the frequency response increases with the increase number of layer from(1 to 2) with percentage (12.91 %), decreases when number of layer increase from (2 to 3) with decreasing percentage (9.65 %), increases with the increase number of layer from(3 to 4) with percentage (15.87 %), decreases when number of layer increase from (4 to 5) with decreasing percentage (6.77 %), increases with the increase number of layer from(5 to 6) with percentage (8.13 %), decreases when number of layer increase from (6to 7) with decreasing percentage (4.80 %), increase with the increase number of layer from(7 to 8) with percentage (5.33 %).

5. CONCLUSION

The delamination problem for typical multi-layer composite plates has been analyzed using finite element method and modal analysis. The study incorporated both computational and experimental work. Comparing the intact and damaged plates, the natural frequencies of plate with delamination are smaller than intact plate. Also, natural frequencies of the damaged plate decrease with the increase of delamination area. The analyses demonstrate that the delamination-induced changes of the plate parameters are mode-dependent. The natural frequency and mode shape effect by damage and size of damage and location of delamination between layers. Boundary condition effect the amount of difference in nature frequency and mode shape and result shown the max. in (CCCC) Bc's, change the number of layers with a thickness constant does not affect the natural frequency of the plate, Whenever damage location close to the center of plate at increase the variation of natural frequency.

RERERENCES

- D. Gay, S. V. Hoa and S. W. Tsai, 2003, *Composite Materials Design and Applications*, Book, CRC Press LLC.
- Gim, C.K.**,** 1994, *Plate Finite Element Modeling of Laminated Plates*, Composite Structure, Vol. **52**, pp.157-168.
- Gobin PF., Jayet Y., Baboux JC., Salvia M, Chateauminois A, Abry JC, et al., 2003, *New Trends in Non-Destructive Evaluation in Relation to the Smart Materials Concept*, Int J Syst Sci ;31(11):1351–9.
- Kayser Aziz Ameen, 2011, Genetic Algorithms FOR Damage DETECTION Of Composite STRUCTURES, the Department of Mechanical Engineering College of Engineering University of Baghdad.
- Metin Aydogdu, and Taner Timarci, 2007, *Free Vibration of Antisymmetric Angle-Ply Laminated Thin Square Composite Plates,* Turkish J. Eng. Env. Sci 31,243-249.
- Mohammed F. Aly, I. G. M. Goda and Gala A. Hassan, 2010, *Experimental Investigation of the Dynamic Characteristics of Laminated Composite Beams*, International Journal of Mechanical & Mechatronics IJMME-IJENS, Vol.(10), No.(03), pp.(59-68).
- Parhi, P.K., Bhattacharyya, S.K. and Sinha, P.K.**,** 2000, *Finite Element Dynamic Analysis of Laminated Composite Plates with Multiple Delaminations*, Journal of Reinforced Plastics and Composites, Vol. **19**, pp. 863-882.
- Shen MH, and Grady JE., 1992, *Free Vibrations of Delaminated Beams*, AIAA J;30(5):1361–70.
- SUDIP DEY and AMIT KARMAKAR, 2011,*Characterization of Multiple Delaminated Composite by Finite Element*, Mechanical Engineering Department, Jadavpur University Kolkata – 700032, West Bengal, India.
- Takeda N., 2000, *Structural Health Monitoring for Smart Composite Structure Systems*, in Japan, Ann Chim-Sci Mat;25(7):545–9.

NOMENCLATURE

$[D]_{s=}$ the elasticity matrix of the s^{th} sub-laminate.
$E_{1,}\, E_{2,}$ *and* E_3 = Young's moduli in direction 1, 2 and 3 respectively N/m^2.
E_{1w}, E_{2w} ,G_{12w} , and υ_{12w} =the mechanical properties of woven fabrics in 1 and 2-directions.
G_{12} = plane shear modulus N/m^2.
G_{13} and G_{23} = transverse shear moduli N/m^2.
h = thickness mm.
k_{xx} k_{yy} k_{xy} = the curvatures of the laminated plate, m^{-1}.

m and f = denote matrix and fiber, respectively.
n_1=number of warp yarns per meter.
n_2= number of fill yarns per meter.
N= number of layers.
N_i = the shape function.
P= number of arbitrarily located delaminations.
u, v, w = displacements in the x,y,z directions respectively for any point, m.
u^0,v^0, w^0 = those at the middle plane of the plate, m.
u_s^0 , v_s^0 = the mid-plane displacements of the s^{th} sub-laminate along x, y.
u_i^0, v_i^0,w_i, θ_{xi}, θ_{yi} = the displacement functions for different nodes.
x_i, y_i = are the co-ordinates of the i^{th} node.
z_s^0 = the distance between the mid-plane of the original laminate and the mid-plane of the arbitrary of s^{th} sub-laminate and the mid-plane of the laminate in z direction mm.
θ_x, θ_y = the rotations of the cross section normal to the y and x axis respectively.
ε^0_{xx}, ε^0_{yy}, γ^0_{xy} = the mid-plane strains
ξ , η = the local isoperimetric co-ordinates of the element.
ξ_i , η_i = the respective values at node i.
σ_{xx}, σ_{yy} = the normal stresses along x and y directions respectively N/m^2.
τ_{xz}, τ_{yz} = the shear stresses in xz, yz planes respectively N/m^2.
υ_{12} , υ_{13}, and υ_{23} = Poisson's ratios.

Table 1. Mechanical properties of fiber and resin, **ref [4].**

Material	Properties	Value
E-Glass fiber	Elasticity modulus (GPa)	74
	Shear modulus (GPa)	30
	Density (kg/m^3)	2600
	Poisson ratio	0.25
Polyester resin	Elasticity modulus (GPa)	4.0
	Shear modulus (GPa)	1.4
	Density (kg/m^3)	1200
	Poisson ratio	0.4

Table 2. Mechanical properties of unidirectional composite material.

Properties	Value
Elastic modulus (E_1) (GPa)	24.7466
Elastic modulus (E_2) (GPa)	6.8989
Shear modulus in plane 1-2 (G_{12}) (GPa)	2.435
Shear modulus in plane 2-3 (G_{23}) (GPa)	2.2211
Poisson ratio in plane 1-2 (υ_{12})	0.3555
Poisson ratio in plane 2-3 (υ_{23})	0.5531

Table 3. Mechanical properties of woven composite material.

Properties	Value
number of warp yarns per meter(n_1)	260
number of fill yarns per meter(n_2)	260
$k=n_1/(n_1+n_2)$	0.5
Elastic modulus ($E_{1w}=E_{2w}$) (GPa)	15.824
Elastic modulus (E_{3w}) (GPa)	8.0181
Shear modulus in plane 1-2 (G_{12w}) (GPa)	2.4355
Shear modulus in plane 1-3 (G_{13w}) (GPa)	2.3232
Shear modulus in plane 2-3 (G_{23w}) (GPa)	2.3232
Poisson ratio in plane 1-2 (υ_{12w})	0.155
Poisson ratio in plane 1-3 (υ_{13w})	0.4937
Poisson ratio in plane 2-3 (υ_{23w})	0.4937

Table 4. Comparison between experimental work and numerical results for four woven layers laminated plate ($[0/90]_4$), with (CCCC) boundary condition.

Case of plate	Results (Hz)	Mode Number				
		1	2	3	4	5
Plate A	Experimental	174.33	378.62	379.83	542.16	811.71
	Numerical	162.88	365.46	365.46	517.77	775.72
	Errors (%)	7.03	3.60	3.93	4.71	4.64
Plate B	Experimental	172.45	347.50	374.42	512.41	792.18
	Numerical	160.75	334.54	358.53	481.31	748.62
	Errors (%)	7.28	3.90	4.43	6.46	5.82
Plate C	Experimental	167.13	341.69	376.63	540.45	747.28
	Numerical	157.25	331.96	364.26	513.85	707.05
	Errors (%)	6.3	2.9	3.4	5.2	5.7

Table 5. Comparison between experimental work and numerical results for four woven layers laminated plate ($[0/90]_4$), with (SSSS) boundary condition.

Case of plate	Results (Hz)	Mode Number				
		1	2	3	4	5
Plate A	Experimental	81.32	225.54	223.79	343.63	508.44
	Numerical	76.165	210.44	210.44	314.31	473.62
	Errors (%)	6.7	7.2	6.3	9.3	7.4
Plate B	Experimental	77.46	203.36	221.82	324.22	499.72
	Numerical	73.081	192.82	206.99	299.14	470.14
	Errors (%)	6.0	5.4	7.1	8.4	6.3
Plate C	Experimental	75.62	209.11	220.06	334.14	481.55
	Numerical	71.85	195.81	209.97	312.88	443.36
	Errors (%)	5.3	6.8	4.8	6.8	8.6

Table 6. Comparison between experimental work and numerical results for four woven layers laminated plate ($[0/90]_4$), with (CFFF) boundary condition.

Case of plate	Results (Hz)	Mode Number				
		1	2	3	4	5
Plate A	Experimental	19.87	32.11	106.96	130.32	146.34
	Numerical	18.447	30.586	100.12	121.11	137.34
	Errors (%)	7.7	4.98	6.83	7.6	6.55
Plate B	Experimental	18.58	30.86	103.23	127.23	144.56
	Numerical	17.814	30.16	99.407	120.11	136.57
	Errors (%)	4.30	2.32	3.85	5.93	5.85
Plate C	Experimental	18.14	30.7	104.19	125.31	140.83
	Numerical	18.26	30.189	98.453	114.64	134.97
	Errors (%)	0.66	1.69	5.83	9.31	4.34

Table 7. Comparison between experimental work and numerical results for four woven layers laminated plate ($[0/90]_4$), with (FFFF) boundary condition.

Case of plate	Results (Hz)	Mode Number				
		6	7	8	9	10
Plate A	Experimental	0	36.45	87.76	99.00	117.09
	Numerical	0	34.889	82.641	92.371	112.39
	Errors (%)	0	4.5	6.2	7.2	4.2
Plate B	Experimental	0	35.40	87.02	97.11	116.69
	Numerical	0	34.295	80.802	88.914	110.08
	Errors (%)	0	3.2	7.7	9.2	6.0
Plate C	Experimental	0	35.02	86.16	95.14	116.21
	Numerical	0	34.26	79.823	87.469	110.41
	Errors (%)	0	2.2	7.9	8.8	5.2

Table 8. Natural frequency **(ω)** of number of layers for cross-ply plates.

Number of layers	stacking sequences	Natural Frequency (ω) (Hz)			
		CCCC	SSSS	CFFF	FFFF
1	0	162.884	76.16456	18.44723	34.88888
2	0/90	161.457	79.72336	17.11052	39.39233
3	0/90/0	162.825	76.49046	18.38476	35.59151
4	0/90/0/90	161.953	80.24534	17.3841	41.23994
5	0/90/0/90/0	162.572	77.9717	18.07511	38.44712
6	0/90/0/90/0/90	162.045	80.34153	17.43333	41.57182
7	0/90/0/90/0/90/0	162.449	78.65752	17.91777	39.57683
8	0/90/0/90/0/90/0/90	162.077	80.37517	17.45046	41.68726

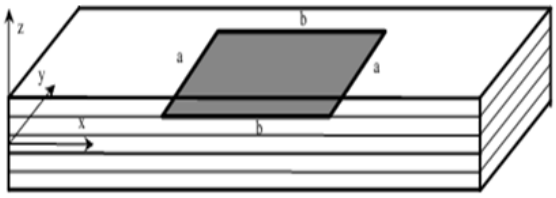

Figure 1. Laminate composite plate with delaminated.

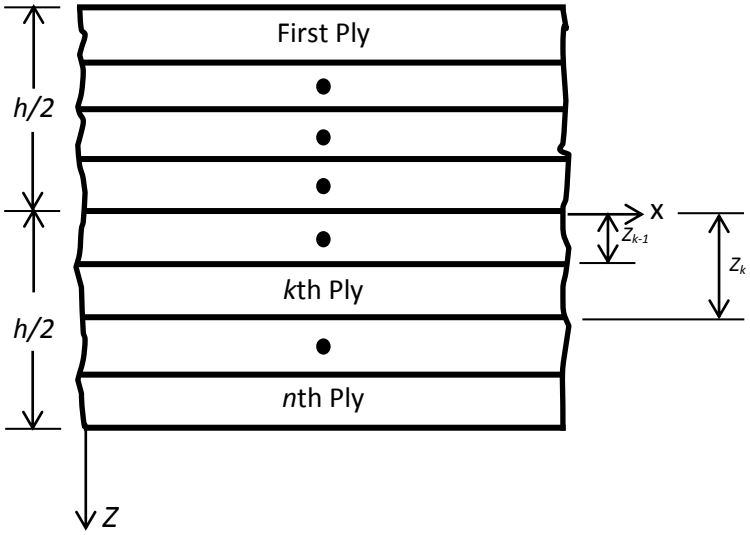

Figure 2. Layer details of the plate.

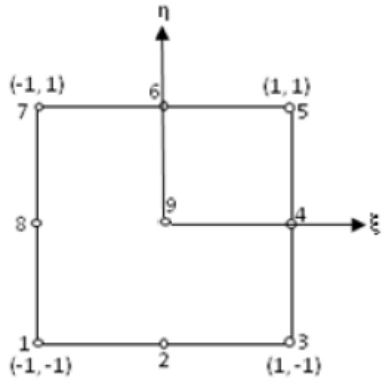

Figure 3. The element in isoperimetric co-ordinates.

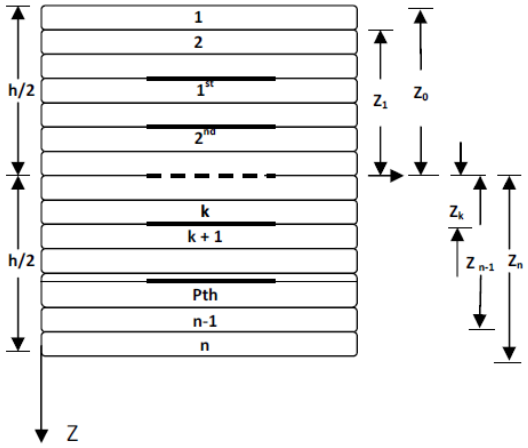

Figure 4. Laminate geometry with multiple delaminations.

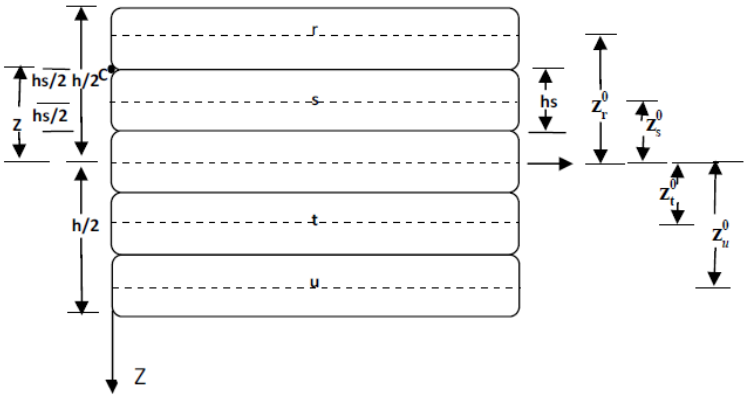

Figure 5. Three arbitrary delaminations leading to four sub-laminates.

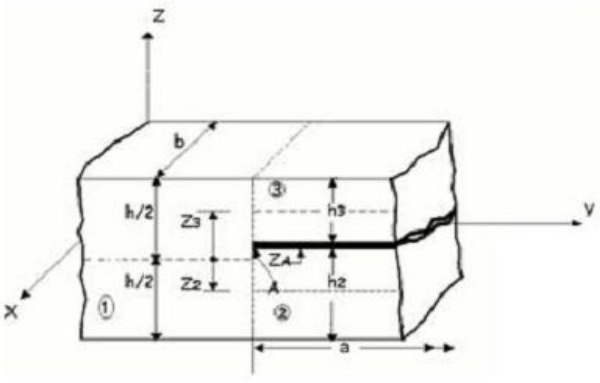

Figure 6. Plate elements at a delamination crack tip **ref.[8].**

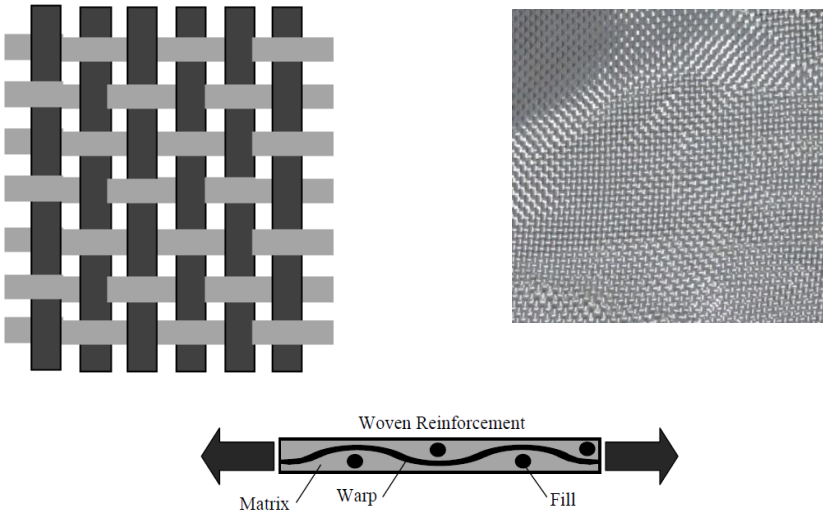

Figure 7. Schematic representation of woven fabric architecture **D. Gay, et al., 2003.**

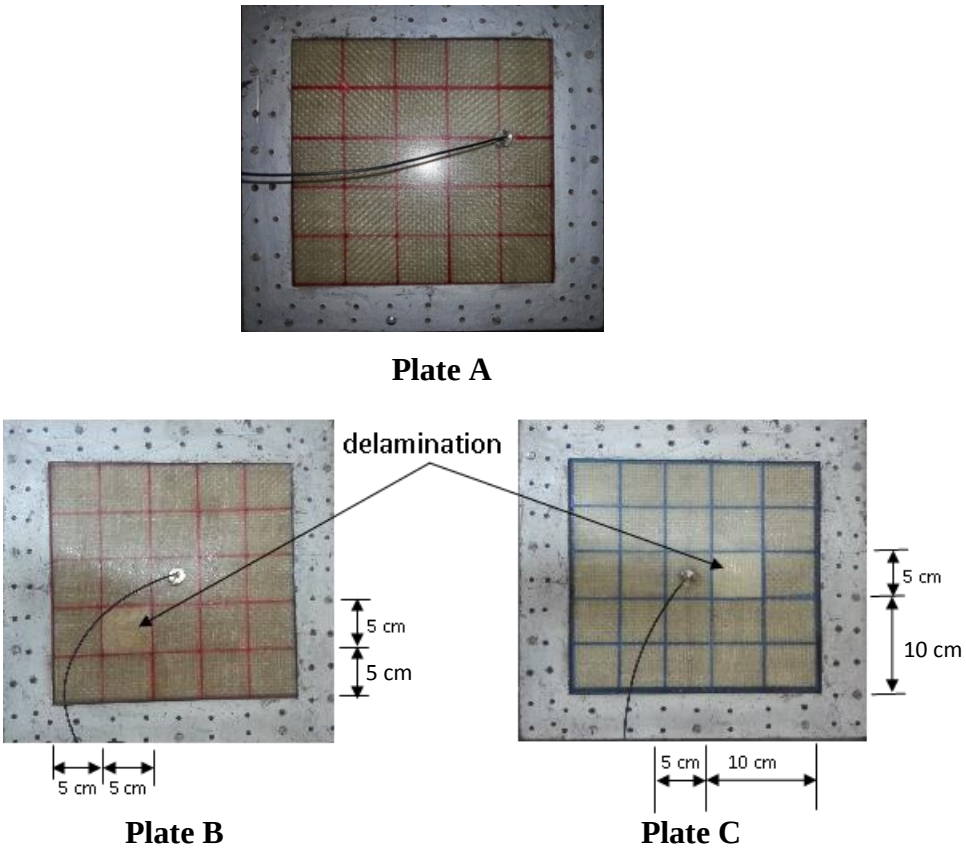

Figure 8. Intact plate and damage plates and clamped all sides.

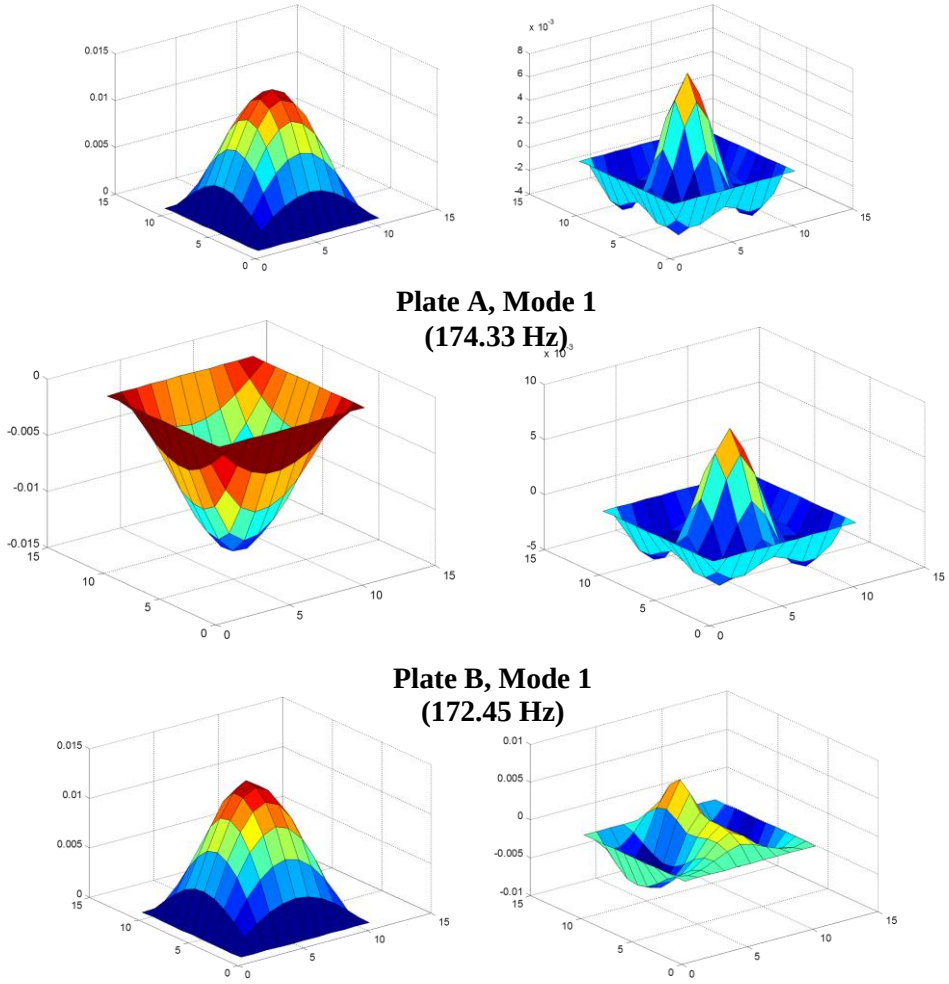

Figure 9. Delamination region in plate A , B and C for some mode shapes of FEM analysis..

Delamination region in plate A , B and C for some mode shapes of FEM analysis